

## Structural Assembly of Multidomain Proteins and Protein Complexes Guided by the Overall Rotational Diffusion Tensor

Yaroslav Ryabov and David Fushman\*

*Contribution from the Department of Chemistry and Biochemistry, Center for Biomolecular Structure and Organization, University of Maryland, College Park, Maryland 20742*

Received February 18, 2007; E-mail: fushman@umd.edu

**Abstract:** We present a simple and robust approach that uses the overall rotational diffusion tensor as a structural constraint for domain positioning in multidomain proteins and protein–protein complexes. This method offers the possibility to use NMR relaxation data for detailed structure characterization of such systems provided the structures of individual domains are available. The proposed approach extends the concept of using long-range information contained in the overall rotational diffusion tensor. In contrast to the existing approaches, we use both the principal axes and principal values of protein's rotational diffusion tensor to determine not only the orientation but also the relative positioning of the individual domains in a protein. This is achieved by finding the domain arrangement in a molecule that provides the best possible agreement with all components of the overall rotational diffusion tensor derived from experimental data. The accuracy of the proposed approach is demonstrated for two protein systems with known domain arrangement and parameters of the overall tumbling: the HIV-1 protease homodimer and Maltose Binding Protein. The accuracy of the method and its sensitivity to domain positioning are also tested using computer-generated data for three protein complexes, for which the experimental diffusion tensors are not available. In addition, the proposed method is applied here to determine, for the first time, the structure of both open and closed conformations of a Lys48-linked diubiquitin chain, where domain motions render impossible accurate structure determination by other methods. The proposed method opens new avenues for improving structure characterization of proteins in solution.

### Introduction

Structural organization of multidomain proteins and protein–protein complexes is a subject of constant interest in structural biology. Structural characterization of these systems, however, presents a significant challenge, because the existing methods for structure determination, X-ray crystallography and nuclear magnetic resonance (NMR), rest on the assumption of a unique conformation and, therefore, could be inadequate when applied to inherently flexible systems. Indeed, domain motions, naturally occurring in a multidomain protein in solution, are completely restricted in crystals. Moreover, packing forces could result in a positioning of protein domains in a crystal structure that might not represent the physiologically relevant conformation (see examples in refs 1–4). NMR has an obvious advantage in that molecules can be studied in their native milieu. The challenges for NMR characterization of multidomain systems are due to the following factors: (1) the conventional NMR approaches based on the nuclear Overhauser effect (NOE) are of limited applicability because of the scarcity of close interatomic contacts between the domains, and (2) the interdomain NOEs that are

observed are often averaged by domain motions, which could render these data uninterpretable.

The introduction of long-range, orientational constraints derived from molecular alignment<sup>5,6</sup> or anisotropy of molecular tumbling<sup>7,8</sup> opened new avenues for structure characterization of macromolecular systems. The orientation-sensitive NMR measurements (spin relaxation, residual dipolar couplings) are uniquely suited for providing structural information about domain organization within a protein, due to the availability of multiple reporter groups (e.g., N–H bonds) with well-defined orientation within each domain. Thus, the concept of orienting domains in a protein based on orientation of the principal axes of diffusion or alignment tensors of the whole molecule “reported” by the individual domains, proposed in refs 1, 9 and schematically illustrated in Figure 1, proved indispensable for structure characterization of multidomain proteins. Provided the structures of individual domains in the monomeric state are available and no significant backbone perturbations occur in the context of the multidomain system, this approach allows proper orientation of the domains in the molecule by a simple rigid-body rotation. Demonstrated examples range from deter-

(1) Fushman, D.; Xu, R.; Cowburn, D. *Biochemistry* **1999**, *38*, 10225–10230.  
(2) Fushman, D.; Cowburn, D. In *Protein NMR for the Millennium*; Krishna, N. R., Berliner, L. J., Eds.; Biological Magnetic Resonance Vol. 20; Kluwer: New York, 2003; pp 53–78.  
(3) Skrynnikov, N.; Goto, N.; Yang, D.; Choy, W.; Tolman, J.; Mueller, G.; Kay, L. *J. Mol. Biol.* **2000**, *295*, 1265–1273.  
(4) Hwang, P. M.; Skrynnikov, N. R.; Kay, L. E. *J. Biomol. NMR* **2001**, *20*, 83–88.

(5) Tolman, J. R.; Flanagan, J. M.; Kennedy, M. A.; Prestegard, J. H. *Proc. Natl. Acad. Sci. U.S.A.* **1995**, *92*, 9279–9283.  
(6) Tjandra, N.; Bax, A. *Science* **1997**, *278*, 1111–1114.  
(7) Bruschweiler, R.; Liao, X.; Wright, P. E. *Science* **1995**, *268*, 886–889.  
(8) Tjandra, N.; Garrett, D. S.; Gronenborn, A. M.; Bax, A.; Clore, G. M. *Nat. Struct. Biol.* **1997**, *4*, 443–449.

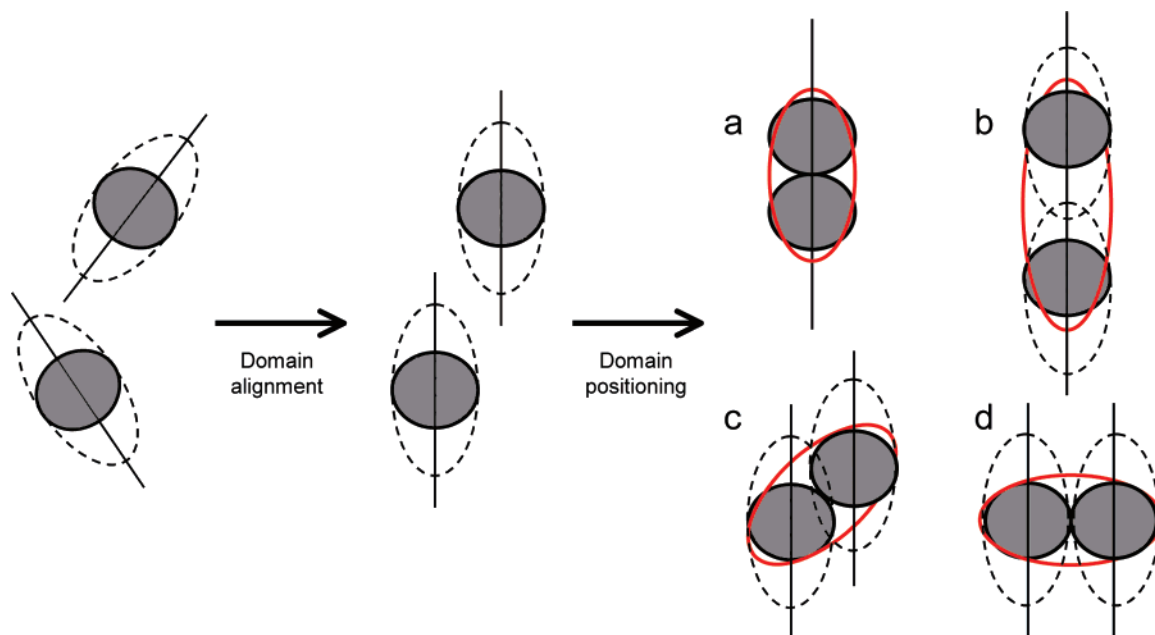


**Figure 1.** Schematic illustration of the proposed concept of domain positioning based on the rotational diffusion tensor. Provided the structures of the individual domains are available, the interdomain orientation is determined first, and domains are oriented by a rigid-body rotation that aligns the corresponding principal axes (shown as sticks) of the overall diffusion tensor of the complex “reported” by the individual domains, as detailed elsewhere.<sup>1,2,10,14</sup> This procedure, however, does not define the relative domain positioning in the molecule. For example, although the interdomain orientation is the same for the domain arrangements (a) through (d), only in (a) is the overall rotational diffusion tensor (red ellipse) consistent with both the magnitude and orientation of the experimental diffusion tensor. In these drawings a dashed ellipse schematically represents the experimentally determined diffusion tensor, whereas a solid red ellipse represents the actual diffusion tensor for a given protein shape/structure. Because the NMR relaxation data sense not only the rate of tumbling but also the orientation of the rotation axes relative to each domain, the relaxation-based approach should be self-sufficient for proper positioning of the domains within a molecule.

mining interdomain orientation in proteins<sup>1,3,4,9–15</sup> to monitoring conformational changes in these systems induced by ligand binding<sup>1,16</sup> or pH conditions.<sup>12,14,15</sup> Despite these advances in determining interdomain orientation in a protein, accurate domain positioning remains a significant challenge, due to the deficiency of the information on the interdomain contacts. This problem can be circumvented by docking approaches<sup>17–20</sup> combining information on interdomain orientation with the interface mapping; the obvious limitation of these methods when applied to multidomain systems is that they imply the existence of a single conformation. Moreover, docking methods are based on surface complementarity and, naturally, have limited applicability when the contact surfaces change in the course of domain movement. It has also been proposed to complement NMR with small-angle scattering data (X-rays or neutrons) in order to address the domain positioning problem.<sup>21,22</sup>

The overall tumbling properties of a molecule in solution reflect its size and shape and therefore contain important information about the domain arrangement within the molecule. Recently developed NMR methods allow accurate measurement of rotational diffusion tensors of proteins.<sup>23,24</sup> In addition, computational approaches are now available for reliable prediction of these tensors directly from protein structures.<sup>25,26</sup> As mentioned above, the existing structural approaches based on diffusion or alignment tensors so far have been focused on determining interdomain orientation. The interdomain distances and relative domain positioning with respect to each other have remained undetermined. This information, critical for complete structure characterization of multidomain systems, is encoded both in the principal values and in the orientation of the overall rotational diffusion tensor. However, it has not been utilized thus far.

Here we extend the concept of using long-range information contained in the rotational diffusion tensor beyond the existing approaches, in order not only to determine the interdomain orientation but also to properly position individual domains relative to each other within a protein or protein complex. We present a simple and robust method of arranging domains in a multidomain system based on its overall rotational diffusion

- (9) Fischer, M. W. F.; Losonczi, J. A.; Weaver, L. J.; Prestegard, J. H. *Biochemistry* **1999**, *38*, 9013–9022.
- (10) Ghose, R.; Fushman, D.; Cowburn, D. *J. Magn. Reson.* **2001**, *149*, 214–217.
- (11) Clore, G. M.; Bewley, C. A. *J. Magn. Reson.* **2002**, *154*, 329–335.
- (12) Varadan, R.; Walker, O.; Pickart, C.; Fushman, D. *J. Mol. Biol.* **2002**, *324*, 637–647.
- (13) Varadan, R.; Assfalg, M.; Haririnia, A.; Raasi, S.; Pickart, C.; Fushman, D. *J. Biol. Chem.* **2004**, *279*, 7055–7063.
- (14) Fushman, D.; Varadan, R.; Assfalg, M.; Walker, O. *Prog. Nucl. Magn. Reson. Spectrosc.* **2004**, *44*, 189–214.
- (15) Ryabov, Y.; Fushman, D. *Proteins* **2006**, *63*, 787–796.
- (16) Evenas, J.; Tugarinov, V.; Skrynnikov, N. R.; Goto, N. K.; Muhandiram, R.; Kay, L. E. *J. Mol. Biol.* **2001**, *309*, 961–974.
- (17) Dominguez, C.; Boelens, R.; Bonvin, A. M. *J. Am. Chem. Soc.* **2003**, *125*, 1731–1737.
- (18) Clore, G. M.; Schwieters, C. D. *J. Am. Chem. Soc.* **2003**, *125*, 2902–2912.
- (19) van Dijk, A. D. J.; Fushman, D.; Bonvin, A. M. *Proteins* **2005**, *60*, 367–381.
- (20) van Dijk, A. D.; Kaptein, R.; Boelens, R.; Bonvin, A. M. *J. Biomol. NMR* **2006**, *34*, 237–244.

- (21) Mattinen, M. L.; Paakkonen, K.; Ikonen, T.; Craven, J.; Drakenberg, T.; Serimaa, R.; Waltho, J.; Annala, A. *Biophys. J.* **2002**, *83*, 1177–1183.
- (22) Grishaev, A.; Wu, J.; Trewthella, J.; Bax, A. *J. Am. Chem. Soc.* **2005**, *127*, 16621–16628.
- (23) Dosset, P.; Hus, J. C.; Blackledge, M.; Marion, D. *J. Biomol. NMR* **2000**, *16*, 23–28.
- (24) Walker, O.; Varadan, R.; Fushman, D. *J. Magn. Reson.* **2004**, *168*, 336–345.
- (25) Garcia de la Torre, J.; Huertas, M. L.; Carrasco, B. *J. Magn. Reson.* **2000**, *147*, 138–146.
- (26) Ryabov, Y. E.; Geraghty, C.; Varshney, A.; Fushman, D. *J. Am. Chem. Soc.* **2006**, *128*, 15432–15444.

tensor. Applications of this method to various proteins demonstrate that, given the structures of individual protein domains, the proposed approach provides a complete characterization of domain organization (orientation and positioning) of a protein, thus fully utilizing the informational content of the overall diffusion tensor.

## Methods

In the method proposed here, individual domains are positioned with respect to each other such that the resulting rotational diffusion tensor provides the best possible match to the experimentally obtained diffusion tensor, as schematically illustrated in Figure 1. For theoretical calculation of the overall diffusion tensor for a given protein structure (domain arrangement) we use an ellipsoidal representation of the protein shape, based on the principal component analysis (PCA) of a solvent-accessible protein surface, implemented in our computer program ELM.<sup>26</sup> The diffusion tensor of such an ellipsoid is then computed using exact equations.<sup>27,28</sup> Comparison with experimental data (NMR, fluorescence) shows that this method provides good accuracy in predicting protein rotational diffusion tensors and is sufficiently fast to be implemented in an iterative search program.<sup>26</sup> This algorithm is implemented in an in-house Matlab program that, for a given structure, compares all components of the overall diffusion tensor,  $D^{\text{calcd}}$ , calculated using PCA, with those of the experimentally measured diffusion tensor,  $D^{\text{exptl}}$ , and searches for the domain arrangement that minimizes the value of the target function:

$$\chi^2 = \sum_{\substack{i=1,3 \\ j=i,3}} (D_{ij}^{\text{calcd}} - D_{ij}^{\text{exptl}})^2 \quad (1)$$

It should be noted that such a criterion simultaneously matches both the principal values and principal axes of  $D^{\text{calcd}}$  and  $D^{\text{exptl}}$ , because the rates and the preferred axes of molecular tumbling both depend on the domain positioning within a molecule. No additional terms (like, e.g., penalty for protein–protein overlap) are currently included in the target function, eq 1; thus the method outlined here should be considered a proof-of-principle rather than a complete structure determination procedure. The current implementation uses a simplex method of exhaustive search in a three-dimensional space of Cartesian coordinates describing the relative position of one domain with respect to the other. The ability to determine relative orientation of the domains independently of this procedure<sup>1,2,10,14</sup> simplifies the search, as only translational degrees of freedom associated with the relative domain positioning are involved.

To evaluate the accuracy of the proposed method and its sensitivity to domain positioning, we applied it here to five protein systems with known domain arrangement. For two of these proteins, HIV-1 protease and maltose binding protein (MBP), the overall rotational diffusion had been characterized experimentally. For HIV-1 protease we used the NMR solution structure published by Yamazaki et al.<sup>29</sup> (PDB code 1BVG) and the components of the rotational diffusion tensor (Table 1) determined by Tjandra et al.<sup>30</sup> For MBP we used the NMR structure derived by Mueller et al.<sup>31</sup> (PDB code 1E2P). The orientation of MBP's rotational diffusion tensor with respect to the molecular reference frame of the protein was not available from the published <sup>15</sup>N relaxation study.<sup>3</sup> Thus, to obtain a complete overall diffusion tensor of MBP we reanalyzed raw NMR relaxation data from that paper<sup>3</sup> (see Supporting Information).

**Table 1.** Comparison of the Diffusion Tensors Derived from Experimental Data (exptl) and Calculated for the Resulting Structures (calcd)<sup>a</sup>

protein	MBP		HIV-1 protease		Ub <sub>2</sub> , closed		Ub <sub>2</sub> , open	
	exptl	calcd	exptl	calcd	exptl	calcd	exptl	calcd
$D_x$ [ $10^7$ s <sup>-1</sup> ]	0.81	0.79	1.33	1.34	1.53	1.60	1.53	1.61
$D_y$ [ $10^7$ s <sup>-1</sup> ]	0.83	0.84	1.41	1.41	1.73	1.61	1.73	1.63
$D_z$ [ $10^7$ s <sup>-1</sup> ]	1.08	1.08	1.85	1.87	2.20	2.28	2.20	2.27
	angles							
$X^{\text{exptl}}$ to $X^{\text{calcd}}$	1.74°		9.65°		5.31°		16.73°	
$Y^{\text{exptl}}$ to $Y^{\text{calcd}}$	1.24°		9.68°		11.95°		27.66°	
$Z^{\text{exptl}}$ to $Z^{\text{calcd}}$	1.31°		0.86°		10.83°		22.01°	

<sup>a</sup> Shown are the principal components of the tensors and the angles between the corresponding principal axes, as indicated.

The testing of the proposed approach also included three protein complexes with unknown overall diffusion tensor parameters: the barnase–barstar complex (PDB code 1BRS<sup>32</sup>); G120R mutant of human growth hormone (hGH) in complex with the extracellular domain of the growth hormone receptor hGHbp (PDB code 1A22<sup>33</sup>); and a complex of protein Z with an in vitro selected affibody (PDB code 1LP1<sup>34</sup>). The rotational diffusion tensors for these complexes (Supporting Information) were predicted from their atom coordinates using the PCA-based method.<sup>26</sup> These computer-generated diffusion tensors were then used to reconstruct the complexes and to explore the values of the target function, eq 1, as a function of the relative displacement of the domains from their original position. Thus these three complexes serve as control examples of protein systems where the diffusion tensors are “known exactly”.

Finally, to demonstrate the utility of our method in the case of domain motions, we analyzed Lys48-linked diubiquitin system, where mutual domain positioning of ubiquitin domains was not characterized thus far. For the individual ubiquitin (Ub) domains in diubiquitin (Ub<sub>2</sub>) we used the NMR solution structure of monomeric Ub determined by Cornilescu et al.<sup>35</sup> (PDB code 1D3Z, where we clipped the flexible C-terminus beyond Arg72). As shown earlier<sup>12,14</sup> the backbone structure of each Ub domain in Ub<sub>2</sub> is practically identical to that of an isolated Ub. The complete rotational diffusion tensor of Ub<sub>2</sub> and the mutual domain orientations at pH 6.8 were obtained previously.<sup>15</sup>

Domain alignment based on the orientations of the principal axes of the overall rotational diffusion tensor has already been described in detail earlier.<sup>1,2,4,10,14,15</sup> Therefore here we address only the problem of domain positioning. Domains in all proteins analyzed here (except for Ub<sub>2</sub> which is a special case discussed below) are considered immobile, and their mutual arrangement in the molecule is known. Thus, in this study we keep the mutual domain orientations in the above complexes fixed (as determined in the original structures<sup>29,31–34</sup> or for Ub<sub>2</sub> in ref 15) and adjust only their relative positioning, by a simple translation of one domain with respect to the other in order to minimize the target function.

Ubiquitin units in Ub<sub>2</sub> exhibit significant reorientations (on a ~10 ns time scale) between two distinct Ub<sub>2</sub> conformations, closed and open, with the former being predominantly populated (90%) at neutral pH.<sup>15</sup> As shown in refs 15 and 36, domain motions in Ub<sub>2</sub> can be described by a simple model of interconversion (exchange) between the two states, while the overall rotational diffusion tensor of the protein remains practically the same for both open and closed states. Thus, in the present analysis we simultaneously positioned Ub domains for both open and

(27) Perrin, F. *J. Phys. Radium* **1934**, *5*, 497–511.

(28) Perrin, F. *J. Phys. Radium* **1936**, *7*, 1–11.

(29) Yamazaki, T.; Hinck, A. P.; Wang, Y. X.; Nicholson, L. K.; Torchia, D. A.; Wingfield, P.; Stahl, S. J.; Kaufman, J. D.; Chang, C. H.; Domaille, P. J.; Lam, P. Y. *Protein Sci.* **1996**, *5*, 495–506.

(30) Tjandra, N.; Wingfield, P.; Stahl, S.; Bax, A. *J. Biomol. NMR* **1996**, *8*, 273–284.

(31) Mueller, G. A.; Choy, W. Y.; Yang, D.; Forman-Kay, J. D.; Venters, R. A.; Kay, L. E. *J. Mol. Biol.* **2000**, *300*, 197–212.

(32) Buckle, A. M.; Schreiber, G.; Fersht, A. R. *Biochemistry* **1994**, *33*, 8878–8889.

(33) Clackson, T.; Ultsch, M. H.; Wells, J. A.; de Vos, A. M. *J. Mol. Biol.* **1998**, *277*, 1111–1128.

(34) Hogbom, M.; Eklund, M.; Nygren, P. A.; Nordlund, P. *Proc. Natl. Acad. Sci. U.S.A.* **2003**, *100*, 3191–3196.

(35) Cornilescu, G.; Marquardt, J. L.; Ottiger, M.; Bax, A. *J. Am. Chem. Soc.* **1998**, *120*, 6836–6837.

(36) Ryabov, Y. E.; Fushman, D. *J. Am. Chem. Soc.* **2007**, *129*, 3315–3327.

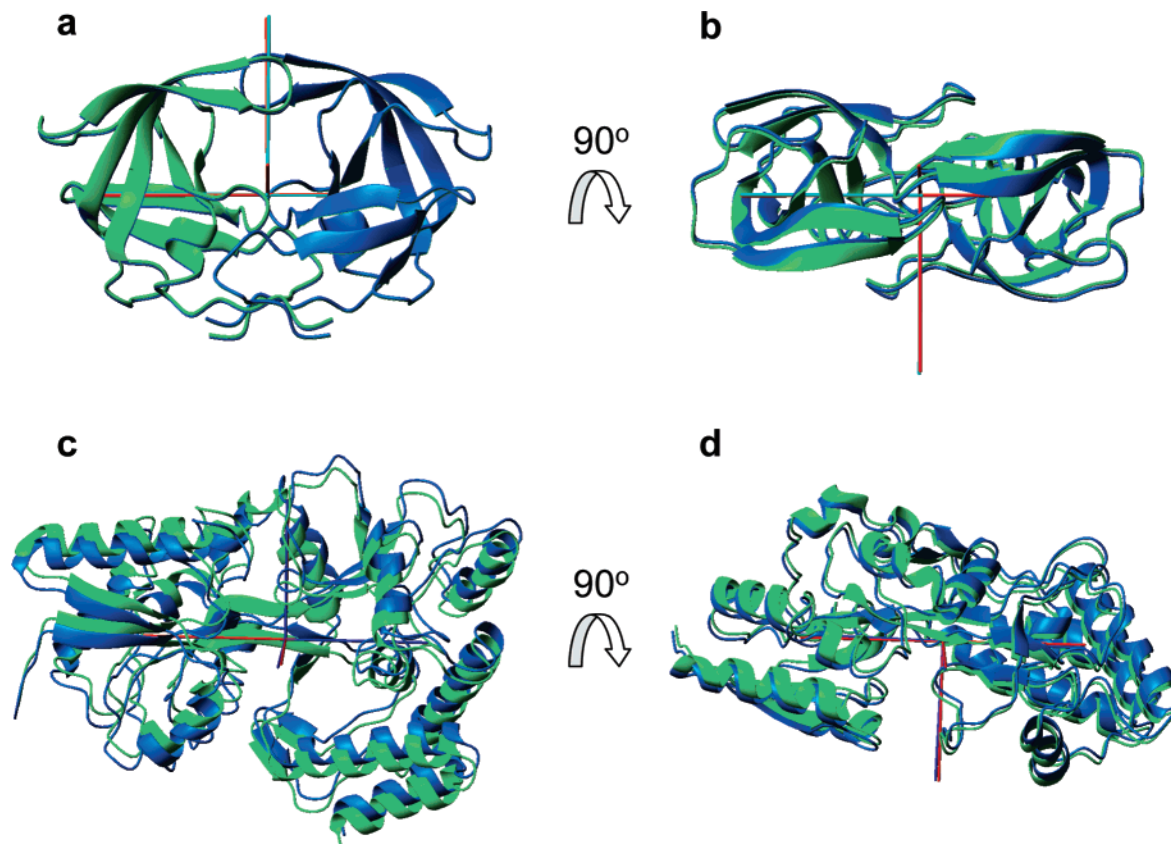


**Figure 2.** Comparison of the structures of (a,b) HIV-1 protease and (c,d) maltose binding protein determined using the proposed method with their NOE-based NMR structures. Shown is the backbone of the original (green) and fitted (blue) structures. To emphasize the relative shift of the domains, these structures are positioned here such that their centers coincide and the relative orientation of the diffusion tensors axes is as obtained from the analysis. Their superimposition minimizing the rmsd between the original and fitted structures is shown in the Supporting Information. Red rods represent the principal axes of the experimentally obtained diffusion tensor, and cyan rods correspond to the principal axes of the diffusion tensors calculated for the resulting structures. All molecular drawings in this paper were made using MolMol.<sup>46</sup>

closed conformations of Ub<sub>2</sub>, and the corresponding contributions to the target function from the two conformations of the chain were weighted by their occupation probabilities.

It should also be noted that hydration of proteins in aqueous solution has a pronounced effect on their diffusion properties. We have shown previously that a monolayer of water molecules covering the surface of a protein can account reasonably well for the available experimental data on rotational diffusion of various proteins.<sup>26</sup> Thus, to model the hydration layer effect we assumed that the surfaces of all proteins in this study are covered with a monolayer of water molecules; i.e., the thickness of the hydration layer in the PCA-based calculations was set to 2.8 Å.<sup>26</sup>

## Results and Discussion

The key idea of the proposed approach is to find the domain arrangement that provides the best possible agreement with the overall rotational diffusion tensor derived from experimental data. This is achieved via an exhaustive search featuring computation of the overall diffusion tensor at each step (see Methods). Until recently, such an approach was impractical because the existing algorithms for prediction of the rotational diffusion tensor from protein structure<sup>25</sup> were too slow to be implemented in an efficient search algorithm. The development of fast methods for diffusion tensor prediction,<sup>26,37</sup> allowing a more than 2 orders of magnitude speedup in calculations, made

it possible to use the overall rotational diffusion tensor as an experimental constraint in protein structure determination.

**Application to HIV-1 Protease and Maltose Binding Protein.** To demonstrate the accuracy of the proposed method we reconstructed the mutual domain arrangement in two different protein systems, the HIV-1 protease and maltose binding protein, for which the three-dimensional structures and experimental diffusion tensors are available (see Methods). HIV-1 protease is a natural homodimer complex. MBP is a single-chain protein that folds into the N-terminal and C-terminal domains comprising residues 6–109 and 264–309 (N-terminal part) and 114–258 and 316–370 (C-terminal part). For each of these proteins, we let the search algorithm find the relative positions of their domains that give the best agreement with the experimentally obtained diffusion tensors. As shown in Figure 2, the proposed method reproduces the domain arrangement in these proteins with remarkable accuracy (see also Supporting Information). The only difference between the original HIV-1 protease structure and the structure obtained by our method is in a small displacement: both HIV-1 domains in the fitted structure are shifted by about 0.5 Å with respect to the original structure (Figure 2a,b). The root-mean-square deviation (rmsd) of 0.36 Å between the original and best-fit structures is within the precision range of the original ensemble of NMR structures that has an rmsd of 0.6 Å. The principal values and the orientation of the principal axes frame of the overall diffusion tensor are both reproduced with very high accuracy (Table 1).

(37) Ortega, A.; Garcia de la Torre, J. *J. Am. Chem. Soc.* **2005**, *127*, 12764–12765.

For MBP, the shift between the original and fitted domain positions (Figure 1c,d) is larger (about 2 Å), although the agreement between the principal values of the experimental and back-calculated rotational diffusion tensors is comparable to that for HIV-1 protease, and even significantly better for the orientations of the diffusion tensor axes (see Table 1). Nevertheless, the rmsd of 1.3 Å between the original and fitted MBP structures is still within the experimental precision of the ensemble of NMR structures, which has the rmsd of 2.3 Å. The greater discrepancy in domain positioning for MBP can be due to several factors. First, the experimental MBP structure has greater structural noise compared to HIV-1 protease. Second, MBP is a 370 residue protein that is about twice as big as the HIV-1 homodimer ( $2 \times 99$  residues). Thus, larger absolute shifts ( $\delta R$ ) in domain positions for MBP could result in smaller relative changes,  $\delta D/D$ , in the overall rotational diffusion tensor (recall that  $D \propto R^{-3}$ , where  $R$  is the “size” of the protein, hence  $\delta D/D \propto \delta R/R$ ). Last but not least, these results could reflect differences in the accuracy and precision of the experimentally determined rotational diffusion tensors for the two proteins. In fact, the diffusion tensors derived from NMR relaxation data are prone to errors originating from the experimental noise as well as from the assumptions made in the data analysis.<sup>14,24,38</sup> For instance, the derivation of the MBP’s diffusion tensor assumed a single rigid structure of the protein, which could be an oversimplification if domain motions are present.

In order to test the performance of our method in the ideal case when the diffusion tensor components are known “exactly”, we repeated the same procedure, this time using the diffusion tensor predicted based on the original structure (instead of the experimental tensor) to guide the assembly of the corresponding proteins. In addition to HIV-1 protease and MBP, we applied this procedure to three protein complexes (see Methods and Supporting Information), for which the experimental diffusion tensors were not available. In all these “ideal” cases, the resulting fitted structures were in excellent agreement with the original structures, with the rmsd values below 0.01 Å (Supporting Information). These results clearly demonstrate the accuracy of the domain positioning approach based on the “true” rotational diffusion tensor.

**Sensitivity to Domain Positioning and Convergence.** The values of the target function ( $\chi^2$ , eq 1) for HIV-1 protease and MBP, plotted as a function of the domain’s displacement (Figure 3a and b, respectively) clearly demonstrate a well-pronounced single minimum corresponding to the optimal domain’s position, which thus justifies the obtained domain arrangement and the stability of the fitting procedure. This conclusion is further supported by similar  $\chi^2$  profiles obtained for the other three protein complexes (see Methods and Supporting Information). In all the cases studied here, displacing one of the domains within a cube with the side of 20 Å centered at the original domain’s position resulted in the convergence to the original structure. Thus, even adopting a very conservative point of view, we can conclude that the proposed method, based on the target function in eq 1, ensures convergence to a single domain arrangement even when the initial domain displacement from the optimal domain arrangement is as big as  $\pm 10$  Å (an interval comparable to the size of a typical protein domain).

Comparing the dependence of the target function,  $\chi^2$ , on domain displacements along the principal axes of the diffusion tensor (Figure 3), it is evident that the sharpest minima correspond to shifts along the Z-axis of the tensor, while noticeably broader minima are associated with domain shifts along the other two axes, X and Y. To quantify this observation, in all examples shown in Figure 3 the estimated confidence intervals in the Z-direction are approximately a factor of 2 narrower than those in the X and Y directions; the latter being comparable with each other (see caption to Figure 3). Note that the principal components of the diffusion tensor are ordered such that  $D_x \leq D_y \leq D_z$ . A shift of one of the domains along the Z-axis, i.e., in the direction of the largest component of the tensor, causes elongation or shortening in the shape of the molecule and, hence, primarily affects the anisotropy,  $A = 2D_z / (D_x + D_y)$ , of the tensor, whereas shifts in the perpendicular directions (X or Y) will primarily alter its rhombicity,  $R = 3A(D_y - D_x) / [2D_z(A - 1)]$ , which reflects deviations from the axial symmetry of the molecule. The sharper  $\chi^2$ -minimum in the Z-direction (Figure 3) suggests that the anisotropy of the overall diffusion tensor is more sensitive to domain positioning than its rhombicity. This observation is in agreement with our computational analysis<sup>26</sup> of a large set of monomeric proteins, which suggests that the anisotropies of diffusion tensors are usually better defined than their rhombicities.

**Diubiquitin Chain Structure.** The results presented above encouraged us to apply the proposed method to Lys48-linked diubiquitin, where the actual structures of the conformers were unknown. At neutral conditions, Ub<sub>2</sub> exists in dynamic equilibrium between two conformations, referred to here as “closed” and “open”, which differ in their occupation probabilities (90% and 10%, respectively) and the relative orientations of Ub domains.<sup>15</sup> Based on the spectroscopic data,<sup>12</sup> the closed conformation of Ub<sub>2</sub> is characterized by a well-defined Ub/Ub interface formed by the hydrophobic surfaces (residues Leu8, Ile44, Val70) of both ubiquitins, while no such interface was detected in the open conformation. In a previous study we determined the relative orientations of Ub domains in both Ub<sub>2</sub> conformers based on their orientation with respect to the principal axes frame of the overall diffusion tensor.<sup>15</sup> We have demonstrated that in the case of Ub<sub>2</sub> the overall tumbling and domain reorientations can be considered statistically independent, to a first approximation, and thus deconvoluted from each other. This is possible because the overall shape of the molecule and hence the overall diffusion tensor remain practically the same for both open and closed states of Ub<sub>2</sub>. That analysis however provided no information about relative positions of the domains with respect to each other. The method proposed here allows us to properly position Ub domains by matching the experimentally determined overall rotational diffusion tensor. Figure 3c shows the profile of  $\chi^2$  as a function of the relative domain positioning in Ub<sub>2</sub>. The resulting structures are shown in Figure 4a,b, and the comparison between the diffusion tensors derived from the experimental data and calculated for the fitted structures is presented in Table 1. It should be mentioned that the difference between the experimental and best-fit tensors for Ub<sub>2</sub> is somewhat bigger than that for the HIV-1 protease and MBP control examples. This reflects a reduced experimental precision in the diffusion tensor of Ub<sub>2</sub>, due to several reasons. First, in order to avoid self-association of Ub<sub>2</sub> the experiments

(38) Fushman, D.; Ghose, R.; Cowburn, D. *J. Am. Chem. Soc.* **2000**, *122*, 10640–10649.

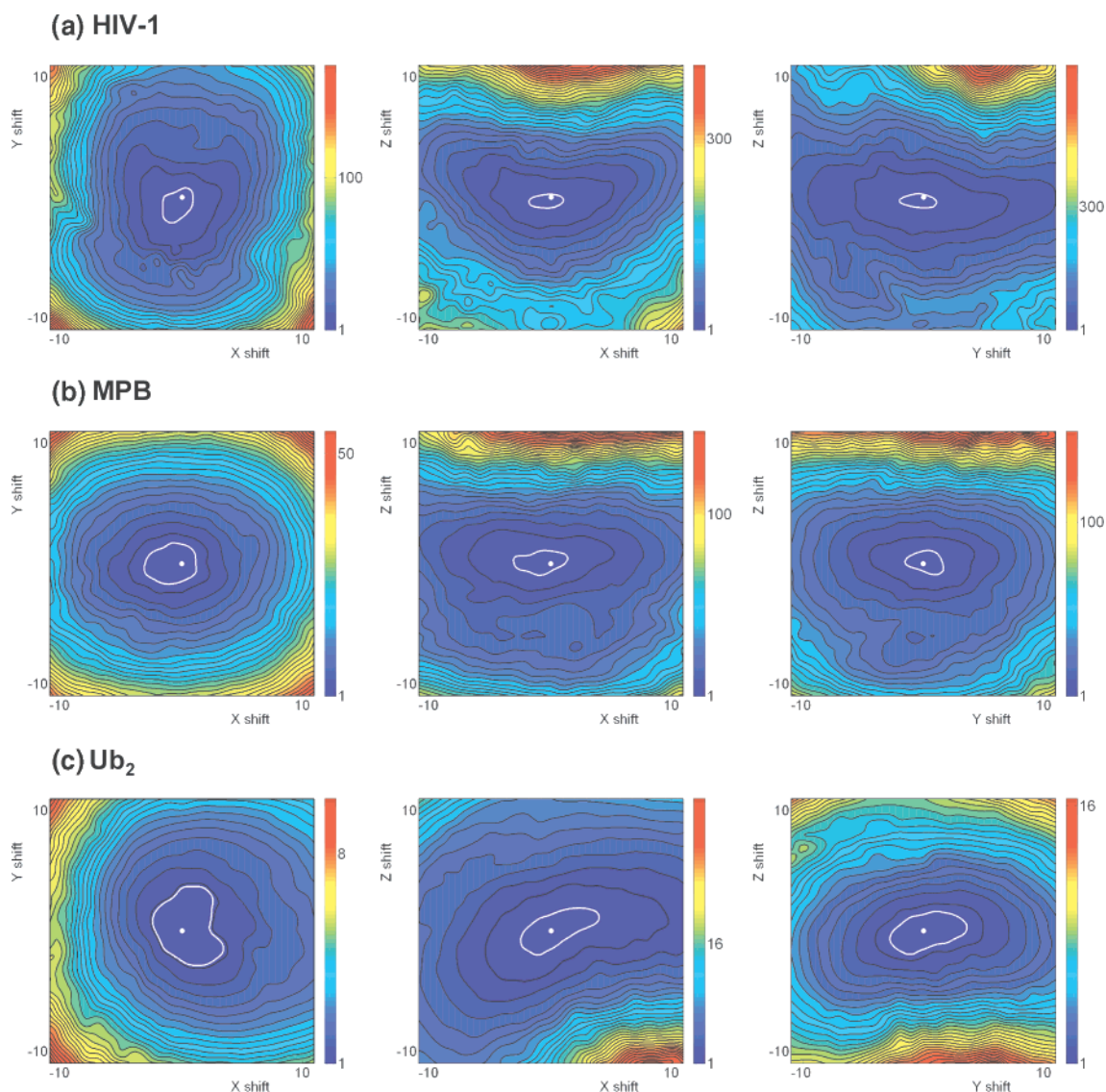


**Figure 3.** Dependence of the normalized target function,  $\chi^2/\chi^2_{\min}$ , on domain displacements (in Å) along the principal axes of the experimentally determined diffusion tensors: (a) for the HIV-1 protease, (b) for MBP, and (c) for Ub<sub>2</sub> at pH 6.8. White dots in the center of each panel mark the location of the  $\chi^2$ -minimum corresponding to the fitted domain positions. White perimeters mark 68% confidence intervals obtained by the  $\chi^2$  boundary method.<sup>47</sup> The estimated confidence intervals (in Å) along the X,Y,Z-axes, respectively, are for HIV-1: [−1.8, 1], [−2, 1], [−1, 0.3]; for MBP: [−3.1, 1.3], [−1.7, 1.7], [−1, 1.1]; and for Ub<sub>2</sub>: [−2.5, 4], [−3.9, 3.7], [−2, 1.9].

were performed at low protein concentrations (250  $\mu\text{M}$ ),<sup>12</sup> which could have affected the precision of the experimental relaxation data. Second, Ub<sub>2</sub> exhibits large-amplitude domain reorientations on a time scale comparable to the overall tumbling. Thus, despite the separability of the corresponding correlation functions,<sup>15,36</sup> the contributions from the overall and domain motions to the measured relaxation rates are convoluted, which inevitably reduces the precision in the derived diffusion tensor. Moreover, due to its low occupation probability ( $\sim 10\%$ ) the open conformation of Ub<sub>2</sub> is less well sampled than the closed conformation. The reduced precision and accuracy of interdomain orientation in the open conformation would then explain the bigger angles between the principal axes of the experimental and best-fit diffusion tensors for this conformation (Table 1). It should be mentioned here that the Ub<sub>2</sub> structures in Figure 4a,b represent an averaged conformation of the chain in each particular state, because any smaller-amplitude interdomain motion present in each of these states would inevitably

be averaged out as a result of an oversimplification introduced by the two-state approximation made in the relaxation data analysis.<sup>36</sup>

**Verification of Diubiquitin Structures.** Unlike the control examples considered above (including HIV-1 protease and MBP), the actual structure of Ub<sub>2</sub> in solution is unknown. However, several lines of evidence suggest that our results are in agreement with the existing experimental data. First, the structure of the closed conformation (Figure 3a) agrees with the chemical shift perturbation data<sup>12</sup> (not included in the calculations here) indicating that residues Leu8, Ile44, and Val70 form the interdomain interface in Ub<sub>2</sub>. Mutations in these residues have been shown to significantly weaken the closed conformation of Ub<sub>2</sub>.<sup>39</sup> Second, the values of the radius of gyration predicted for the Ub<sub>2</sub> structures in Figure 4a,b using CRYSOLE<sup>40</sup> (17.3–17.9 Å and 17.0–17.6 Å for the closed and

(39) Varadan, R.; Assfalg, M.; Raasi, S.; Pickart, C.; Fushman, D. *Mol. Cell* **2005**, *18*, 687–698.

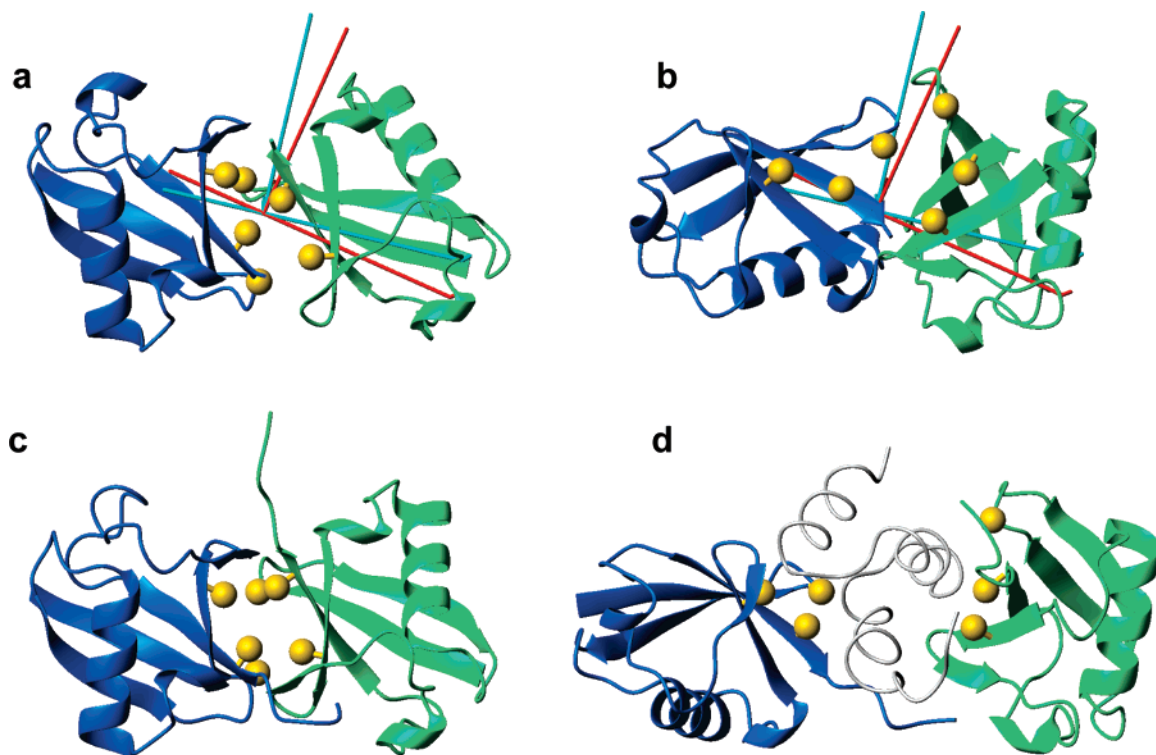


**Figure 4.** Structures of the (a) closed and (b) open conformations of Lys48-linked Ub<sub>2</sub> at pH 6.8 obtained using the proposed approach and their comparison with the existing structural data: (c) the crystal structure<sup>42</sup> of Ub<sub>2</sub> at pH 4.5 and (d) the solution structure of the Ub<sub>2</sub>/UBA complex<sup>39</sup> at pH 6.8 (the UBA domain is shown as a thin gray ribbon). The distal domain is colored blue, and the proximal domain is green. The location of the hydrophobic patch residues Leu8, Ile44, and Val70 of both Ub domains is shown in a ball-and-stick representation (C<sub>β</sub> atoms, colored gold). In panels (a) and (b), the rods represent the principal axes of the experimentally determined diffusion tensor (red) and the diffusion tensor calculated for the resulting structures (cyan). Flexible C-terminal residues 73–76 are not shown in (a), (b). Note that no constraints related to direct interdomain interaction were included in the calculations shown here.

open conformers, respectively) are in excellent agreement with the value  $17.4 \pm 0.8$  Å experimentally determined by small-angle X-ray scattering.<sup>41</sup> Third, the derived structures are also in agreement with the paramagnetic relaxation enhancements observed in the proximal Ub domain as a result of site-directed paramagnetic spin labeling of the distal domain.<sup>14,15</sup> The reconstructed position of the unpaired electron of the spin label (see ref 15 for details), based on the closed conformation, is at a distance of 8.2 Å from the C<sub>α</sub> atom of residue 48 of the distal Ub, in good agreement with its expected location (Supporting Information). Last but not least, in both Ub<sub>2</sub> structures, the flexible C-terminus of the distal Ub (not shown in Figure 4a,b) is positioned sufficiently close to Lys48 of the proximal Ub in order to form the isopeptide bond between the two Ub domains in Ub<sub>2</sub> (note that no constraints were included in the calculation to reflect the presence of the Ub–Ub linker).

It is also instructive to compare the Ub<sub>2</sub> structures obtained here with those observed under different conditions: the crystal structure of Ub<sub>2</sub> (PDB code 1AAR<sup>42</sup>) and the Ub<sub>2</sub> complex with the C-terminal UBA domain of hHR23a (PDB code 1ZO6<sup>39</sup>). As one can see from comparison of Figure 4a,b with Figure 4c,d, these latter structures resemble the closed and open conformations of Ub<sub>2</sub> derived by our method. Indeed, a direct superimposition (not shown) gives a fair agreement between

the closed conformation of Ub<sub>2</sub> in solution obtained here and the Ub<sub>2</sub> crystal structure, with the backbone rmsd of 2.4 Å for the elements of secondary structure. Most important for the proposed method is that our calculation placed the two Ub units at a distance very similar to that in the crystal structure, with the centers of mass of the ubiquitins being 23.0 Å apart in Figure 4a and 23.4 Å apart in Figure 4c. The difference in domain orientation between the two structures can be represented as a 30° rotation of one of the domains with respect to the other (or 10° rotation for the distal and 21° for the proximal), which is within the precision of the interdomain orientation in the closed conformation.<sup>15</sup> It should be pointed out that Ub<sub>2</sub> is inherently flexible and its conformation in solution is pH-dependent.<sup>12,15</sup> Therefore, the closed conformation of Ub<sub>2</sub> at pH 6.8 in solution is not expected to match exactly the structure of the chain in crystals grown at a different pH (pH 4.5). The fact that no closed conformation has been observed in solution at pH 4.5<sup>12</sup> suggests that the crystal structure of Ub<sub>2</sub> could be a result of crystal packing forces. Taking this into consideration together with the fact that no information about interdomain contacts was included in our calculation, the observed agreement between the two structures is remarkable.

A comparison with the structure of the Ub<sub>2</sub>/UBA complex (Figure 4d) reveals structural/mechanistic details of the conformational changes in Ub<sub>2</sub> accompanying UBA binding. In particular, the UBA insertion shifted Ub units away from each other compared to their equilibrium positions in the unbound Ub<sub>2</sub>: the distance between the centers of the ubiquitins increased from 22.3 Å in the open conformation (Figure 4b) or 23.0 Å in

(40) Svergun, D. I.; Barberato, C.; Koch, M. H. J. *J. Appl. Crystallogr.* **1995**, *28*, 768–773.

(41) Tenno, T.; Fujiwara, K.; Tochio, H.; Iwai, K.; Morita, E. H.; Hayashi, H.; Murata, S.; Hiroaki, H.; Sato, M.; Tanaka, K.; Shirakawa, M. *Genes Cells* **2004**, *9*, 865–875.

(42) Cook, W. J.; Jeffrey, L. C.; Carson, M.; Zhijian, C.; Pickart, C. M. *J. Biol. Chem.* **1992**, *267*, 16467–16471.

the closed (Figure 4a) to 35.4 Å in the complex (Figure 4d). In addition, UBA binding to the open Ub<sub>2</sub> conformation is accompanied by a 43° rotation of the distal and 30° of the proximal domain, and the total interdomain reorientation angle is 70°. The corresponding UBA-induced reorientations in the closed conformation are 24° for the distal Ub and 46° for the proximal, or 69° total. To further characterize the conformational transition involved in UBA binding, we analyzed these structures using DynDom.<sup>43</sup> The analysis indicates that domain rearrangement in the closed conformation of Ub<sub>2</sub> (Figure 4a) upon UBA binding can also be visualized as a combination of a 5.4 Å translation and a 68° rotation of one of the ubiquitins (e.g., proximal) about an axis which is parallel to the Ub/Ub interface (99.7% a closure axis) and goes through the Ub–Ub linker (K48 in the proximal domain), acting as a hinge in the process of interface opening.

**Utility of Rotational Diffusion Tensor as a Structural Constraint.** The results presented above demonstrate that the overall rotational diffusion tensor can be used for structure determination of multidomain proteins and protein complexes. The uniqueness of the approach proposed here is based on the diffusion tensor's sensitivity to the overall shape of the protein and on the availability of a large number of structurally well-defined reporter groups within each domain. Because spin relaxation senses both the axes of molecular tumbling and the corresponding rates, the relaxation-based approach could be self-sufficient for proper orientation and positioning of the domains within a molecule. For example, even in the case of spherically shaped individual domains, when the structures (a), (b), and (d) in Figure 1 are all characterized by the same overall tumbling time (and the principal values of the diffusion tensor), their rotational diffusion tensors are distinct, when expressed in the same coordinate frame. This is due to the fact that the NMR relaxation data report not only on the rate of tumbling but also on the orientation of the rotation axes relative to each domain.

The approach described here assumes that (1) the structure of the individual domains is known (e.g., is essentially the same as of the isolated domains) and (2) the domains tumble together as a single moiety and not as completely independent “beads on a flexible string”; i.e. the description of the system with the common overall rotational diffusion tensor is physically meaningful. The validity of these assumptions for a particular multidomain system requires verification, as discussed in detail elsewhere.<sup>2,14</sup> It is worth pointing out in this regard that, despite the large-amplitude opening/closing interdomain dynamics in Ub<sub>2</sub>, to a good approximation the two domains do tumble and orient together, as inferred from <sup>15</sup>N relaxation data and residual dipolar couplings.<sup>12</sup>

The time scale of interdomain motion is an important factor to be considered when applying the proposed method to flexible systems. If this motion is much faster than the overall tumbling, the latter will be characterized by an averaged (over all available conformations) diffusion tensor, and the information on the relative interdomain orientations will be averaged too. Therefore  $D^{\text{calcd}}$  in eq 1 should represent a common diffusion tensor averaged over the diffusion tensors calculated for different interconverting conformations. In the opposite case, when the exchange is comparable to or slower than the overall tumbling (as in the case of Ub<sub>2</sub> considered here), the diffusion tensor is

not averaged, and it makes sense to characterize each conformation by its diffusion tensor. Thus one has to fit the calculated diffusion tensor for each conformation to its experimental diffusion tensor (available, for example, from relaxation data analysis), and this procedure is expected to yield meaningful structural information about the interconverting states.

The usefulness of the diffusion tensor as a structural constraint could be placed in a wider context, beyond its application to multidomain systems demonstrated here. Because of the sensitivity to the overall size and shape of the protein, the diffusion tensor-based “long-distance” constraints can also be used to improve general structure characterization for monomeric proteins. As demonstrated in ref 8, the orientation dependence of <sup>15</sup>N relaxation rates can be used as orientational constraints for structure refinement of anisotropically tumbling monomeric proteins. The ability to evaluate the diffusion tensor at virtually every step of protein structure calculation<sup>26</sup> now opens the possibility to use both the orientation and the principal values of the tensor to drive the resulting structure to closely match the actual size and shape of the protein. Combined with the site-specific relaxation data, this could allow a more accurate orientation of the individual groups with respect to the overall shape of the protein. In addition, the inclusion of the diffusion tensor as a constraint could help improve the compactness of NMR-derived protein structures,<sup>44</sup> which is currently achieved by including a radius-of-gyration-based term in structure refinement. Unlike the radius of gyration, which is a scalar shape-nonspecific measure of the global size of the molecule, the diffusion tensor contains structural information specific to both the size and shape of a protein.

## Conclusions

Here we presented a novel approach to structure characterization of multidomain systems based on structural information encoded in the rotational diffusion tensor. The results demonstrate that the full informational content of the overall rotational diffusion tensor can be used for structure determination of multidomain proteins and protein complexes. This includes not only the orientation of the domains but also their relative positioning within the molecule. The feasibility of this approach is demonstrated here for five protein systems, where our method reproduced their structures with very high accuracy. Detailed testing of the proposed method shows that it ensures convergence of the fitting procedure to a single domain arrangement in those situations when the initial uncertainty in domain positioning is less than or comparable to the domain dimensions.

It should be emphasized that the proposed method provides a unique possibility for structure characterization of protein systems with significant domain mobility, which might not be amenable to other, more conventional structural methods, like X-ray crystallography, NOE- and RDC-based NMR methods, and docking approaches. In fact, the application of this method to Lys48-linked diubiquitin allowed us to determine, for the first time, the structure of the open and closed conformations of this chain in solution and obtain a detailed picture of conformational changes in Ub<sub>2</sub> induced by ligand binding. Thus, the proposed approach could become the method of choice for structure characterization of inherently flexible systems, like multidomain proteins and weakly bound protein complexes.

(43) Hayward, S.; Berendsen, H. J. *Proteins* **1998**, *30*, 144–154.

(44) Kuszewski, J.; Gronenborn, A. M.; Clore, G. M. *J. Am. Chem. Soc.* **1999**, *121*, 2337–2338.



The current implementation of the method merely matches the experimental and predicted diffusion tensors, and therefore, the results presented here should be considered as a proof-of-principle. A more accurate, high-resolution structure calculation would require combining diffusion tensor information with other structural constraints (e.g., from NOEs, RDCs, contact surface mapping etc), as well as the proper force field potentials accounting for the van der Waals, electrostatic, and other interactions. This can be achieved by incorporating our approach into the existing structure determination and docking protocols, which should be relatively straightforward and will be our future goal.

The proposed concept could, in principle, be extended to domain positioning based on residual dipolar couplings resulting from molecular alignment. Indeed, in the case of steric forces, the molecular alignment reflects the shape of the molecule and, therefore, should be sensitive to the relative positioning (not only orientation) of the domains. Computational tools for predicting molecular alignment based on the structure have been developed.<sup>45</sup> The situation is complicated here by the tracelessness of the alignment (Saupe) tensor, which introduces an

arbitrary scaling factor into the experimentally determined principal values of the tensor. It should be possible, however, to use ratios (free of this scaling factor) of the principal components of the alignment tensors in a similar way to that described in this paper.

**Acknowledgment.** Supported by NIH grant GM065334 to D.F. We thank Prof. Nikolai Skrynnikov for kindly providing the experimental NMR relaxation data for MBP, and Dr. Jennifer B. Hall for critical reading of the manuscript. Atom coordinates for the Ub<sub>2</sub> conformations have been deposited with the Protein Data Bank (ID codes: 2PEA, 2PE9). The software used in this study will be available from the authors upon request.

**Supporting Information Available:** Parameters of the overall rotational diffusion tensor obtained for MBP from the experimental data; a figure depicting superimposition of the original and fitted structures of HIV-1 protease and MBP; a figure demonstrating the dependence of the target function on domain arrangement for 1BRS, 1A22, and 1LP1 structures; a table listing the diffusion tensor parameters predicted for these structures accompanied by a figure showing the orientation of the corresponding diffusion tensor axes; and a figure presenting validation of the derived structure of the closed conformation of Ub<sub>2</sub> using site-specific spin labeling. This material is available free of charge via the Internet at <http://pubs.acs.org>.

JA071185D

(45) Zweckstetter, M.; Bax, A. *J. Biomol. NMR* **2002**, *23*, 127–137.

(46) Koradi, R.; Billeter, M.; Wuthrich, K. *J. Mol. Graphics* **1996**, *14*, 51–55.

(47) Press, W. H.; Teukolsky, S. A.; Vetterling, W. T.; Flannery, B. P. *Numerical Recipes in C*; Cambridge University Press: New York, 1992.